Resonance Model Comparison for High-Frequency AC Link Three-port Converter

1st Julien Allard
Inst. of Mechatronic, Electrical Energy, and Dynamic Systems, UCLouvain
Louvain-la-Neuve, Belgium
julien.Allard@umons.ac.be

2nd Eduardo Vasquez Mayen
Inst. of Mechatronic, Electrical Energy, and Dynamic Systems, UCLouvain
Louvain-la-Neuve, Belgium
eduardo.vasquez@uclouvain.be

3rd Emmanuel De Jaeger
Inst. of Mechatronic, Electrical Energy, and Dynamic Systems, UCLouvain
Louvain-la-Neuve, Belgium
emmanuel.dejaeger@uclouvain.be

***Abstract*—The interest in High-frequency AC (HFAC) link converters has increased with the rise of renewable energies, the needed energy storage to complement the energy production, and electric vehicles. In this context, HFAC link converters have been proposed as an elegant multiport converter solution that allows connecting energy sources, energy storage, and electric vehicels with a single converter. The operating frequency at which the HFAC link will operate depends on the power to be transferred and the resonance time of this link. In this paper, three different methods for calculating the resonance time and their impact on the total frequency of the converter are investigated. By applying simplifications, this work demonstrates that accurate results are achievable while reducing the complexity of the calculation. Based on these simplifications, less complex analytical models of the converter can be derived.**

***Index Terms*—soft-switching, inverters, high-frequency AC link converter.**

I. Introduction

The energy transition has led to the growing use of renewable energies such as photovoltaics (PVs) and batteries as a complementary production elements. Additionally, there has been an increase in the use of electric vehicles (EVs) which represent a significant power demand. Therefore, coupling PVs directly with EVs has been proposed as an intuitive solution. The connection among these different elements requires the use of multiple converters. In this context, the High-frequency AC (HFAC) link converters have a promising application. This type of converter allows the connection of multiple elements simultaneously. This advantage eases the interconnection between the PVs, batteries, and loads using a single converter. The converter can be considered an extension of a buck-boost converter where a capacitor is placed in parallel with the inductor. The parallel LC circuit, referred to as the HFAC link, allows the converter to adjust its voltage for each source or load, by allowing a resonance during small periods refered to as ”resonance periods”. After the resonance, the corresponding port is connected to the HFAC link and charges or discharges the HFAC link inductance for a specific period of time to transfer power. The HFAC link also has as advantages the capability for bi-directional power flow, and the reduction in the size and weight of heat dissipating components [1], [2].

The converter architecture, first introduced in [3], has been implemented as an AC/AC and AC/DC buck-boost converter for medium voltage applications [4]. In other studies, the converter has been used to connect PV inverters and PV strings to their loads [5]–[7]. The converter capabilities as a multiport system were shown in [8], [9]. The use of the HFAC link as a three-port converter has also been proposed for efficient delivery of energy to electric vehicle charging terminals in [10]. In the literature, the resonance periods are often neglected to simplify the computation of the link frequency and port periods. However, under certain conditions, these simplifications are no longer valid. An incorrect estimation of the frequency can lead to incorrect periods for each source/load. Thus, creating errors in the average power transferred among the ports of the converters. Therefore, validating which simplifications can be used and under which conditions is important.

In this paper, a comparison between three methods for calculating the converter operation frequency is presented. Among these methods, one neglects the resonance periods, the second method uses simplified expressions for the resonance periods, and the final method considers the resonance periods without any simplifications. The objective of the comparison is to asses under which conditions the resonance periods have a significant impact on the link frequency and thus cannot be neglected in the analysis. The results show that the model considering the resonance with some simplifications is close to the results of the most detailed method without significant deviations. In Section II the operating principle of the converter will be detailed. The three different frequency computation methods are presented in Section III. Section IV presents the case study and the obtained results. Finally, the conclusions will be given in Section V.

II. Converter Operating principle

The converter studied is an extension of the buck-boost converter. By adding a capacitor in parallel to the inductance, an HFAC link is formed. To transfer power, the link inductor is charged by the sources and discharged towards the loads. The

This work was done in the context of the project MIRaCCLE (Micro-réseau Industriel avec Raccordement en Courant Continu et Luminaires Extérieurs), and supported by the government of the Région Wallonne of Belgium.

frequency of the HFAC link is significantly higher than that of the converter ports. Thus, the converter can also connect to AC devices or the main AC grid. The circuit diagram of the studied converter is shown in Fig. 1 where the switches (S_1,S_2,...,S_8) represent bidirectional switches.

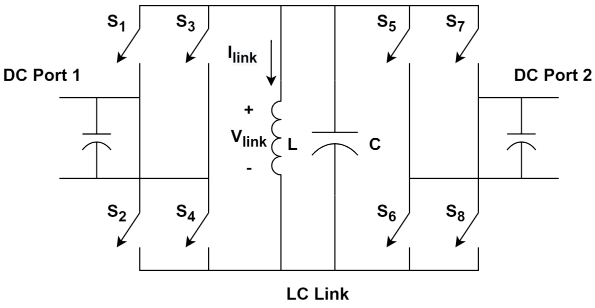

Fig. 1. Circuit diagram of a two-port HFAC link converter.

This converter topology has several advantages. Firstly, the converter is a quasi-square wave zero-voltage switching converter. This implies that the switches start conducting only when the voltage across their terminals is zero. Thus, reducing the switching losses. Another advantage is that the converter has two power cycles per period. A power cycle is a full charge and discharge cycle of the energy stored in the inductor. The second power cycle is achieved by allowing the link to charge and discharge with opposite polarity. This second power cycle reduces the resonance time during which no energy is transferred. It also leads to an increase in the efficiency of the converter. Finally, the proposed architecture allows for bidirectional energy transfer in any port with the possibility of having either DC or AC devices connected. The basic operating principle for a two-port DC/DC converter is presented hereafter:

Mode 1: Link Charge During this first mode illustrated in Fig. 2, the source connected to Port 1 will charge the AC link. This connection is done via switches S_1 and S_4. The switches of the port supposed to charge the link during mode 1 start conducting once the link voltage reaches the highest input voltage. This is so that the switching occurs at zero voltage. The inductance is then charged until the current reaches its reference value. Based on the high frequency of the link, it is considered that the voltage at the input port remains constant during this mode. From the inductance voltage equation, it is possible to calculate the link current as shown in (1).

$$i_{Link} = \frac{1}{L}\int_0^t V\,dt = \frac{V(t)}{L} + i_{Link}(0) \tag{1}$$

Mode 2 and 4: Partial resonance Between each charge or discharge mode, there is a resonance mode as shown in Fig. 3. During this time, no switch is conducting. The HFAC link will resonate causing the voltage to change. The resonance will end when the zero-voltage condition is satisfied. The HFAC link can be described by the following equations:

$$i_C = -i_{Link} = C\frac{dV_{Link}}{dt} \tag{2}$$

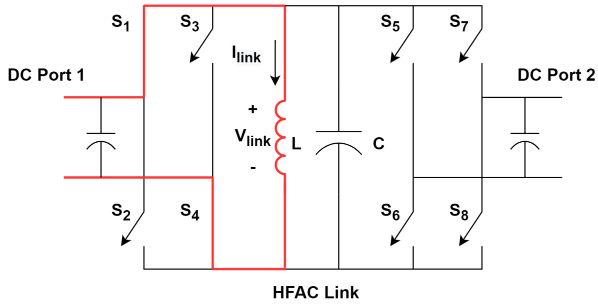

Fig. 2. Circuit diagram of the converter during Mode 1.

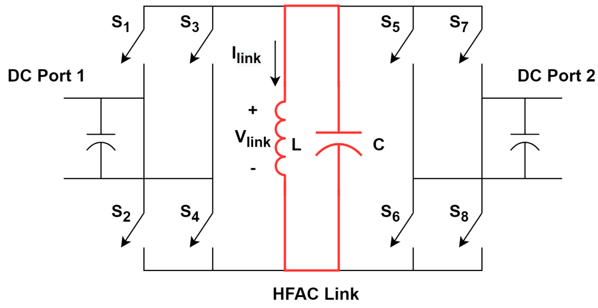

Fig. 3. Circuit diagram of the converter during Modes 2 and 4.

$$V_{Link} = L\frac{di_{Link}}{dt} \tag{3}$$

Mode 3: Link Discharge The energy stored in the link is discharged towards Port 2 via the switches S_5 and S_8. There is a certain amount of energy left in the link inductance. This energy is needed for the link to swing back to a predetermined voltage that is higher than the maximum input voltage. This mode is shown in Fig. 4.

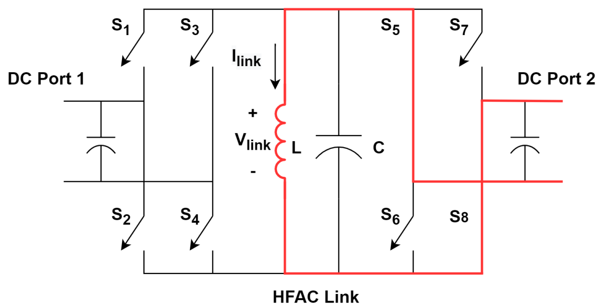

Fig. 4. Circuit diagram of the converter during Mode 3.

Mode 3 would be followed by Mode 4. In other words, another resonance mode where the voltage will swing back to the predetermined highest voltage. This resonance is then followed by a set of modes having the same behavior as modes 1 through 4 except that the link would charge and discharge with opposite polarity. Therefore, in this case, the complementary switches on the legs would be used.

The operating principle for a three-port converter, shown in Fig. 5, is highly similar. To illustrate this example, it is considered that Port 1 and Port 3 will provide power to Port 2 and that the voltage of Port 3 is higher than that of Port 1. The operating principle of the converter will be as follows. As Port 3 has the highest voltage, Port 3 will be the first to charge the inductance. This would be followed by a resonance mode. After the resonance, Port 1 would begin to charge the inductance until it reaches its reference value. Another resonance mode will occur. Finally, the inductance is discharged towards Port 2. One final resonance would occur where the HFAC link would swing to the highest voltage. After this, the process would be repeated but with the link charging and discharging in the reverse direction. The evolution of the HFAC link current and voltage during this process are illustrated in Fig. 6.

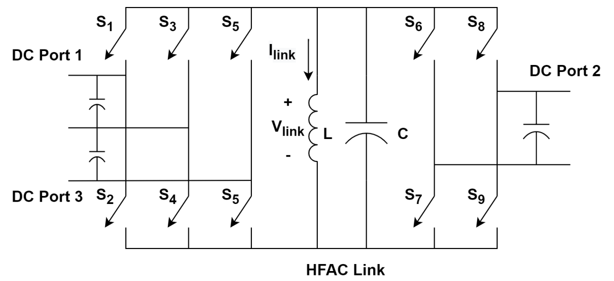

Fig. 5. Circuit diagram of a three-port HFAC link converter.

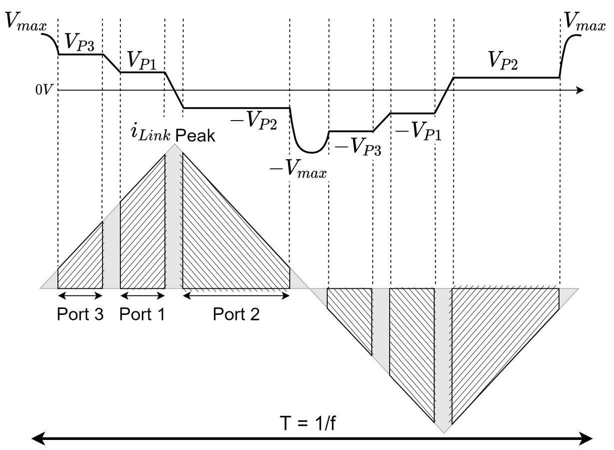

Fig. 6. Three-port converter AC link voltage and current waveform.

III. HFAC LINK FREQUENCY COMPUTATION

An important parameter of the converter is the HFAC link operating frequency. This frequency is influenced by the power rating of the converter, the link charge and discharge times, and the duration of the resonance modes. As shown before, several resonance modes occur throughout a period of the converter. In some cases, these resonance periods can be significantly smaller than the total converter period. Thus, these resonance periods can be neglected in the calculations to reduce the complexity. Here, three different methods for the calculation of the link frequency and the resonance time are presented. These methods are compared and their impact on the calculation of the link frequency will be studied. The objective is to assess in which regimes the resonance periods have a significant impact on the HFAC link frequency. The three proposed methods are:

- *Neglected resonance*: The general analysis of the converter does not consider the resonance periods [9].
- *Reduced order*: Only the resonating periods during the power cycle are considered. This means the resonance between the end of a power cycle and the start of the next one is neglected. The computation is done using a reduced order calculation [11].
- *High order*: This method considers all the resonating periods during the power cycle. This method gives the closest results to the actual operating values [12].

Neglected resonance

In this method it is assumed that once connected, the voltage of the port does not vary, the equation of the inductor for each mode i is:

$$V_{i+1} = L\frac{I_{i+1} - I_i}{t_{i+1}} \tag{4}$$

Where t_i is the duration of the mode. Taking into account the trapezoidal waveform of the link current, the average current transferred through the converter can be calculated as:

$$I_{i+1,avg} = t_{i+1}(I_{i+1} + I_i)f \tag{5}$$

Where f corresponds to the frequency of half a power cycle. Considering n sources and m loads with two power cycles per period, the following relationship is obtained:

$$\sum_{i=0}^{n+m-1} t_{i+1} = \frac{1}{2f} \tag{6}$$

Using the voltage and average current expressions, and considering that the initial current is equal to zero, it is possible to link the power exchanged and the peak current of the link. This relation is shown in (7).

$$\sum_{i=0}^{n-1} P_{i+1} = LfI_{L,peak}^2 = P_{in} = -\sum_{i=n}^{n+m-1} P_{i+1} \tag{7}$$

By using (4) and (7), the expression for the peak current in the Link can be found as shown in (8) with $P_0 = 0$ [9]. Finally, by using (7), the frequency of the link based on the power and inductance can be found. The resulting equation is shown in (9).

$$I_{L,peak} = 2 * \sqrt{P_{in}} \sum_{i=0}^{n+m-1} \frac{\sqrt{\sum_{i=0}^{i} P_{i+1}} - \sqrt{\sum_{i=0}^{i} P_i}}{V_{i+1}} \tag{8}$$

$$f = \frac{P_{in}}{LI_{L,peak}^2} \tag{9}$$

Once the frequency is found and through the help of the previous equations, it is possible to calculate the duration of each mode through the following equation:

$$t_{i+1} = \frac{L}{f}\frac{\sqrt{\sum_{i=0}^{i} P_{i+1}} - \sqrt{\sum_{i=0}^{i} P_i}}{V_{i+1}},\ i = 0, 1, 2, ..., n-1 \quad (10)$$

Reduced order

As previously mentioned, the HFAC link behaves as an LC oscillator whose behavior can be described by (2) and (3). The *Reduced order* method relies on the assumption that the link current will not vary during the resonance mode, and only the voltage will change. With these assumptions, the resonance time can be calculated as:

$$V_{Link}(t_2) - V_{Link}(t_1) = -\frac{I_1 * t_{res}}{C} \quad (11)$$

$$t_{res} = C\frac{V_{Link}(t_2) - V_{Link}(t_1)}{I_1} \quad (12)$$

I_1 corresponds to the link current before the resonance mode at time t_1. $V_{Link}(t_1)$ is the link voltage at the beginning of the resonance mode, and $V_{Link}(t_2)$ is the link voltage at the end of the resonance mode. Through an iterative process, the resonance period calculated using (12) is added to the duration of the other conduction modes to obtain the frequency of the link. The duration of the modes is recomputed using this new frequency, and the process is stopped when the change between iterations is small ($\sim 1Hz$).

High order

For an accurate result, none of the previous assumptions are taken into account. This means that both the voltage and the current are considered to vary during the resonance modes. At the end of the discharge mode, there has to be a current left in the HFAC link to enable the voltage swing. This current I_{end} can be calculated as shown in (13) where V_{max} is maximum voltage to which the link swings and V_{last} is the voltage of the last port to be connected. The current left in the link at the beggining of the first mode is called I_1. I_1 can be calculated as shown in (14) where V_{first} is the voltage of the first port to be connected and ω_r is the resonance angular frequency given by $1/\sqrt{LC}$. In this case, the duration of the resonance is given by (15) [12].

$$I_{end} = \sqrt{\frac{C}{L}(V_{max}^2 - V_{last}^2)} \quad (13)$$

$$I_1 = \sqrt{\left(I_{end} + \left(\frac{V_{last}}{L\omega_r}\right)^2 - \left(\frac{V_{first}}{L\omega_r}\right)^2\right)} \quad (14)$$

$$t_{r1} = \frac{1}{\omega_r}\left(\pi + \tan^{-1}\left(\frac{I_1 L\omega_r}{V_{first}}\right) - \pi + \tan^{-1}\left(\frac{I_{end}L\omega_r}{V_{last}}\right)\right) \quad (15)$$

While this method provides an acurrate solution, it has a higher numerical complexity as the function is non-linear. This non-linearity can increase the computation time and increase the complexity of the models to be derived.

IV. Results

To test the accuracy of the different methods, the calculation of the link frequency for the different methods is performed in MATLAB and is compared. The case presented in Fig. 7 is studied. PVs are connected to Port 1 and feed a load connected to Port 3. A battery is connected to Port 2. The power injected by the PVs and the consumption of the load change at each step. The power injected by the PVs changes from $1kW$ to $30kW$. Meanwhile, the load increases from $0.9kW$ to $15kW$. The battery charges with the exceeding power injected by the PVs. In Fig. 7, it is shown that there are three resonance periods per power cycle. As depicted in 7, the complete cycle of the converter is described as:

$$\frac{1}{2f} = t_{Port1} + t_{res1} + t_{Port3} + t_{res2} + t_{Port2} + t_{res3} \quad (16)$$

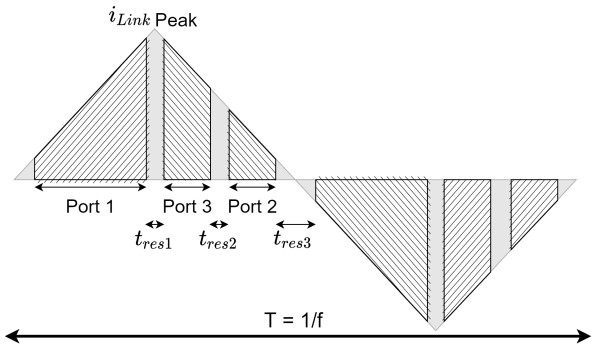

Fig. 7. Link current waveform for Port 1 feeding Port2 and Port3.

In (16), t_{res1} is the resonance period between Port1 and Port 3. t_{res2} is the resonance period between Port3 and Port2. t_{res3} is the resonance occurring before the voltage swing to the voltage of Port 1. In the *High order* method, all of these resonance periods are considered. Meanwhile, the last resonance period t_{res3} is neglected in the *Reduced order* approach. The parameters used for the calculations are given in Table I.

TABLE I
Converter Parameters

Parameter	Value
Port 1 Voltage [V]	300
Port 2 Voltage [V]	400
Port 3 Voltage [V]	200
Link inductance [μH]	140
Link capacitance [nF]	200
Maximum power [kW]	30

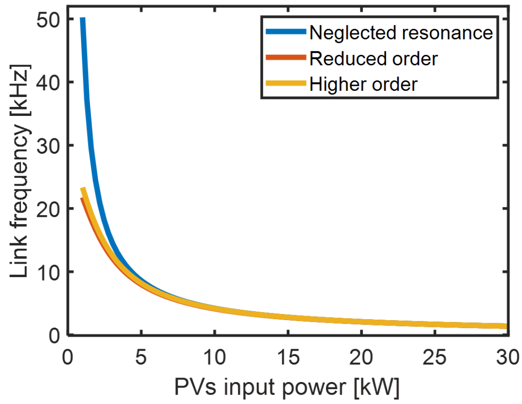

Fig. 8. Link frequency calculated by each method at different power levels.

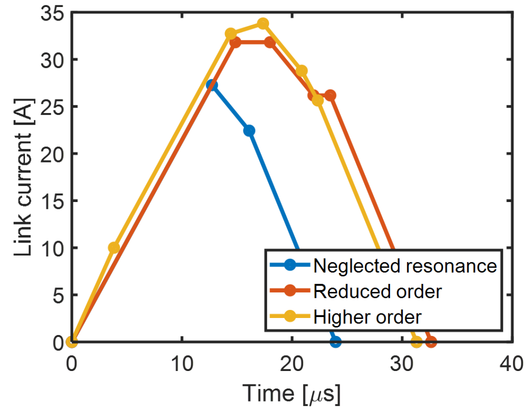

Fig. 9. HFAC link current waveform with $2.17kW$ input power.

The obtained results are shown in Fig. 8. When the power injected by the PVs increases, the link frequency decreases. The three curves follow the same profile except at low power. At low power levels, the method neglecting the resonance deviates significantly from the other two methods. Indeed, when the power transferred is low, the duration of resonance is comparable to or even longer than the transfer time [6]. Therefore, neglecting the resonance results in a frequency deviation from the more elaborated methods. In contrast, the *Reduced order* method shows a slight underestimation of the link frequency at low power levels.

To further illustrate this deviation in frequency, the waveform of the HFAC link current is drawn. Fig. 9 shows the waveform when the power injected by the PVs is $2.17kW$ and the load demands $1.47kW$. The *Higher order* model has an additional starting point which corresponds to I_1, which is the leftover current on the link. The current in the *Reduced order* method stays constant during the resonance periods as it is one of the simplifications made. The waveform of the *Neglected resonance* method reflects the difference in the calculated frequency. At this power level, the resonance times are significant, and thus neglecting them leads to a different result. This is because the current fed to the link is low. Hence, the duration of the port connection is short. In contrast, the duration of the resonance remains relatively constant.

Fig. 10 is the HFAC link waveform when the PVs provide $8.03kW$ and the load demands $4.31kW$. At this point, the duration of the resonances is small enough compared to the connection time of each port. Thus, it is seen that the three different models follow a similar waveform.

As it was shown in Fig. 8, the *Reduced order* method at lower power levels is more accurate than the method neglecting the resonance periods. The percentage of error of the *Neglected resonance* and *Reduced order* methods can be calculated by considering the most rigorous *High order* method as the reference. However, the degree of error in each method also depends on the voltage difference between each port. The error is calculated for each method for two voltages in Port 1: $300V$ and $600V$.

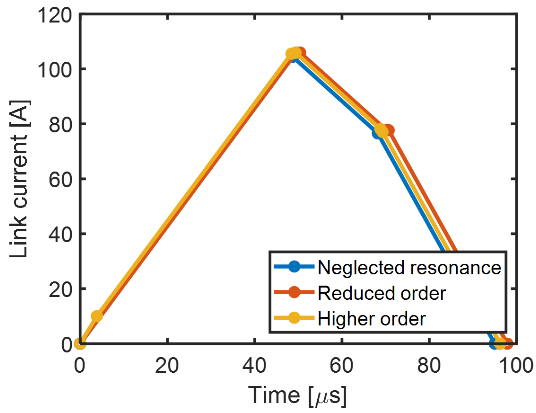

Fig. 10. HFAC link current waveform with $8.03kW$ input power.

Fig. 11 shows the error percentage for the most simple method. As seen previously, the amount of error at low power levels is non-negligible. The error starts at 115% with $300V$ and 250% for $600V$. The error then decreases towards a negligible value.

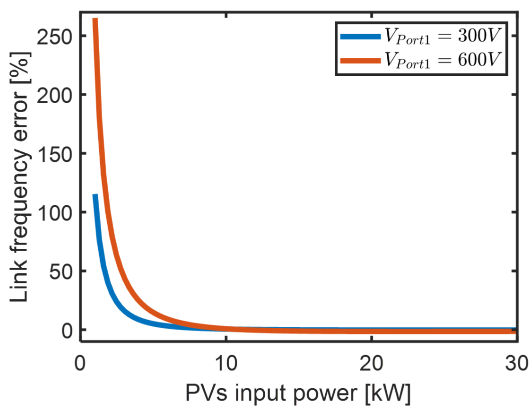

Fig. 11. Link frequency calculation error with Neglected resonance method.

The error obtained with the *Reduced order* method is shown in Fig. 12. It is seen that the error starts close to 5% when the voltage of Port 1 is $300V$. When the voltage is $600V$, the error increases towards 15%. However, this increased error is significantly less than with the *Neglected resonance* method. The increased error due to the voltage change can be explained by noticing that the voltage at the end of the cycle ($V_{Port2} = 400V$) is lower than the input voltage ($V_{Port1} = 600V$). When this is the case, the link no longer discharges to zero. The current left in the link is used to increase the link voltage back to the input voltage.

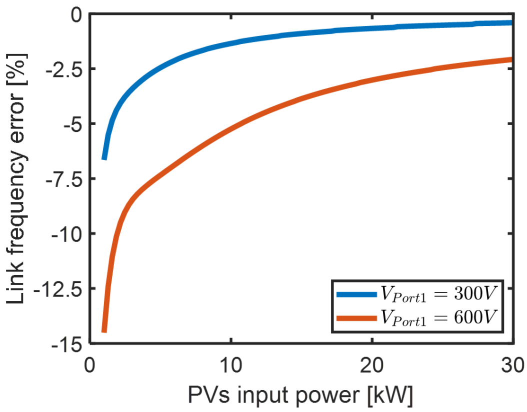

Fig. 12. Link frequency calculation error with Reduced order method.

In Fig. 13 the duration of each resonance period with respect to the total period is shown. This result is obtained using the higher order method as the presence of a third resonance period suggests. During normal power operation, the duration of the final resonance period is more significant than the duration of the resonance periods between the charge and discharge of the link. This last resonance corresponds to the resonance that creates the voltage swing at the end of each power cycle. This results indicates that $t_{res,1}$ and $t_{res,2}$ can be neglected. Meanwhile, the last resonance $t_{res,3}$ could be kept to improve the accuracy of the result.

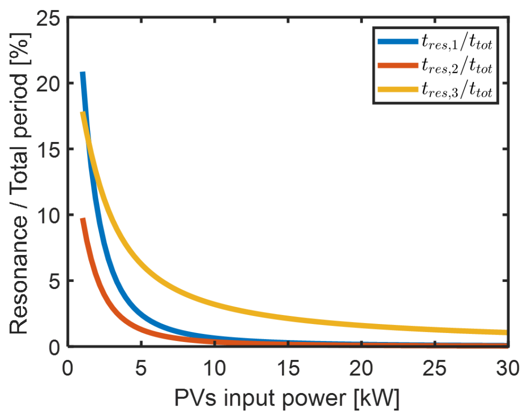

Fig. 13. Duration of the resonance periods with respect to the total period.

V. Conclusion

This paper presents a comparison among three different methods for the calculation of the operation frequency of a HFAC link converter. The operation principles for a two-port converter and a three-port converter were shown. The results show that under low power levels the most simple method has a significant error. However, the lower order method provides a more accurate result with reduced complexity. The behavior of the resonance periods with the *High order* method was shown. It was seen that under normal operation the intermediate resonance periods have a negligible duration, but to obtain more accurate results the final resonance period could be considered.

In future work, a mathematical model of the converter will be developed using the simplifications and validations found. These mathematical models could be used to derive averaged models to allow a fast simulation of such type of converter.

References

[1] P. Sood, T. Lipo, and I. Hansen, "A versatile power converter for high frequency link systems," in *1987 IEEE Applied Power Electronics conference and Exposition*. San Diego, CA USA: IEEE, Mar. 1987, pp. 249–256.

[2] P. Sood and T. Lipo, "Power conversion distribution system using a high-frequency AC link," *IEEE Transactions on Industry Applications*, vol. 24, no. 2, pp. 288–300, Apr. 1988.

[3] A. Balakrishnan, H. A. Toliyat, and W. C. Alexander, "Soft switched ac link buck boost converter," in *2008 Twenty-Third Annual IEEE Applied Power Electronics Conference and Exposition*. Austin, TX, USA: IEEE, Feb. 2008, pp. 1334–1339.

[4] H. A. Toliyat, A. Balakrishnan, M. Amirabadi, and W. Alexander, "Soft switched ac-link AC/AC and AC/DC buck-boost converter," in *2008 IEEE Power Electronics Specialists Conference*. Rhodes, Greece: IEEE, Jun. 2008, pp. 4168–4176.

[5] M. Amirabadi, A. Balakrishnan, H. A. Toliyat, and W. Alexander, "Soft switched ac-link direct-connect photovoltaic inverter," in *2008 IEEE International Conference on Sustainable Energy Technologies*. Singapore, Singapore: IEEE, Nov. 2008, pp. 116–120.

[6] M. Amirabadi, A. Balakrishnan, H. A. Toliyat, and W. C. Alexander, "High-Frequency AC-Link PV Inverter," *IEEE Transactions on Industrial Electronics*, vol. 61, no. 1, pp. 281–291, Jan. 2014.

[7] J. Sadeghi, E. F. Choolabi, and M. H. Zare, "A new topology of unidirectional multistring PV inverter with high frequency AC-Link," in *2016 24th Iranian Conference on Electrical Engineering (ICEE)*. Shiraz, Iran: IEEE, May 2016, pp. 1254–1259.

[8] M. Amirabadi, H. A. Toliyat, and W. C. Alexander, "A Multiport AC Link PV Inverter With Reduced Size and Weight for Stand-Alone Application," *IEEE Transactions on Industry Applications*, vol. 49, no. 5, pp. 2217–2228, Sep. 2013.

[9] A. Alfares, S. A. K. H. Mozaffari Niapour, and M. Amirabadi, "High frequency AC microgrid based on a highly reliable single-stage converter," in *2015 IEEE Energy Conversion Congress and Exposition (ECCE)*. Montreal, QC: IEEE, Sep. 2015, pp. 2361–2367.

[10] R. Dosquet, D. Rixhon, and P. Bleus, "Future local intelligent transactional energy node for ev charging and mobility hub," in *CIRED Porto Workshop 2022: E-mobility and power distribution systems*, vol. 2022, 2022, pp. 965–969.

[11] W. C. Alexander, "Universal power converter with bidirectional switching devices," U.S. Patent US8345452B2, 2009.

[12] M. Amirabadi, J. Baek, H. A. Toliyat, and W. C. Alexander, "Soft-Switching AC-Link Three-Phase AC–AC Buck–Boost Converter," *IEEE Transactions on Industrial Electronics*, vol. 62, no. 1, pp. 3–14, Jan. 2015.